Elasticity of Pseudomonas putida KT2442 Surface Polymers Probed with Single-Molecule Force Microscopy

ARTICLE *in* LANGMUIR · APRIL 2002

Impact Factor: 4.46 · DOI: 10.1021/la015695b

2 AUTHORS:

Nehal I Abu-Lail
Washington State University
46 PUBLICATIONS **1,080** CITATIONS

SEE PROFILE

Terri A Camesano
Worcester Polytechnic Institute
93 PUBLICATIONS **2,396** CITATIONS

SEE PROFILE

Elasticity of *Pseudomonas putida* KT2442 Surface Polymers Probed with Single-Molecule Force Microscopy

Nehal I. Abu-Lail and Terri A. Camesano*

Worcester Polytechnic Institute, Department of Chemical Engineering, 100 Institute Road, Worcester, Massachusetts 01609

Received November 25, 2001. In Final Form: February 21, 2002

Single-molecule force microscopy was used to study the effect of solvent polarity and ionic strength on the elasticity of bacterial surface polymers. Adhesion forces were measured between *Pseudomonas putida* KT2442 bacterial cells and silicon nitride tips of an atomic force microscope (AFM). Force−extension profiles were analyzed to determine the elasticity of the polymer chains in several solvents (water, formamide, methanol, 0.1 M KCl, and 0.01 M KCl). Adhesion peaks were fit to entropic-based, statistical mechanical, random walk formulations (the freely jointed chain (FJC) and the wormlike chain (WLC) models). The experimental data showed better agreement with the FJC (average $R^2 = 0.86 \pm 0.20$) than the WLC model (average $R^2 = 0.76 \pm 0.22$). The segment length was 0.18−1.0 nm in all five solvents using the FJC model, with about 60% of the chains having a segment length of 0.154−0.20 nm. The persistence length was 0.18−0.83 nm using the WLC model, with about 78% of chains having a persistence length of 0.154−0.20 nm. The WLC model was not able to represent polymer properties for chains of <11 nm (4% of the data), since persistence lengths shorter than the C−C bond were obtained. The WLC model also failed to predict the high-magnitude adhesion forces in KCl solutions and methanol. The extensible freely jointed chain model (FJC+) was considered since the latter accounts for enthalpic effects neglected in the FJC model, but it did not represent the data better than the FJC model. Adhesive interactions between the biopolymer and the AFM tip were compared in these solvents. Adhesion was highest in the least polar solvent, methanol. Adhesion forces in water and formamide were about the same and less than forces observed in methanol. Although biopolymer contour lengths varied over a wide range (tens to hundreds of nanometers) in all solvents, shorter lengths were observed when salt was present, indicating that the polymer chains were less extended in the presence of salt.

Introduction

Understanding bacterial adhesion to surfaces requires knowledge of the conformational properties of bacterial surface polymers.[1−5] Bacterial surface and extracellular polymers play a role in biofilm properties and dynamics, such as the induction of genetic changes,[1] the development of microbial consortia,[6] the enhanced resiliency of cells to antibiotics, chlorination and other potential disinfectants,[7−9] and corrosion.[10] Biofilm formation is also important in environmental bioremediation,[11,12] drinking water quality, and biomedical applications such as adhesion to contact lenses[13] and other implanted or prosthetic devices.[5,14,15] While it is known that bacterial surface macromolecules play a role in bacterial adhesion and biofilm formation, very little is known regarding the physical properties of these biopolymers on a single-molecule basis.

Earlier results indicated that bacterial adhesion to surfaces may be controlled by polymer interactions.[16−20] Lipopolysaccharides (LPS) cover 45% of the surface of Gram-negative bacteria[21] and may protrude 30 nm or more into the surrounding media.[4] Many bacterial surfaces also have a layer of extracellular polysaccharides (EPS).[6] Some correlation with biopolymer size and adhesion has been observed. For example, the affinity of *Escherichia coli* and *Citrobacter freundii* O-antigens for TiO_2 and Al_2O_3 surfaces increased as the molecular mass of the O-antigen increased.[17] Polymer compressibility and affinity for solids were thought to determine whether polymers enhanced

* To whom correspondence should be addressed. Phone: (508) 831 5380. Fax: (508) 831 5853. E-mail: terric@wpi.edu.

(1) Fletcher, M.; Decho, A. W. Biofilms. *Encyclopedia of Life Sciences*; Nature Publishing: New York, 2001.
(2) Courvoisier, A.; Isel, F.; François, J.; Maaloum, M. *Langmuir* **1998**, *14*, 3727.
(3) van der Aa, B. C.; Michel, R. M.; Asther, M.; Zamora, M. T.; Rouxhet, P. G.; Dufrêne, Y. F. *Langmuir* **2001**, *17*, 3116.
(4) Jucker, B. A.; Zehnder, A. J. B.; Harms, H. *Environ. Sci. Technol.* **1998**, *32*, 2909. Jucker, B. A.; Harms, H.; Zehnder, A. J. B. *Colloids Surf., B* **1998**, *11*, 33.
(5) Nablo, B. J.; Chen, T.-Y.; Schoenfisch, M. H. *J. Am. Chem. Soc.* **2001**, *123*, 9712.
(6) Davies, D. G.; Parsek, M. R.; Pearson, J. P.; Iglewski, B. H.; Costerton, J. W.; Greenberg, E. P. *Science* **1998**, *280*, 295.
(7) Fletcher, M. *Adv. Microb. Physiol.* **1991**, *32*, 53.
(8) Marshall, K. C. Adhesion as a strategy for access to nutrients. In *Bacterial Adhesion*: *Molecular and Ecological Diversity*; Fletcher, M., Ed.; Wiley: New York, 1996; pp 59−87.
(9) Fletcher, M. (Ed.) Bacterial attachment in aquatic environments: a diversity of surfaces and adhesion strategies. In *Bacterial Adhesion*: *Molecular and Ecological Diversity*; Fletcher, M., Ed.; Wiley: New York, 1996; pp 1−24.
(10) Dexter, S. C. *Biofouling* **1993**, *7*, 97.
(11) Decho, A. W. *Oceanogr. Mar. Biol.* **1990**, *28*, 73.
(12) Scharmm, A.; Larsen, L. H.; Revsbech, N. P.; Ramsing, N. B.; Amann, R.; Schleifer, K. H. *Appl. Environ. Microbiol.* **1996**, *62*, 4641.
(13) Serry, F. M.; Revenko, I.; Allen, M. J. Application note. Digital Instruments: Santa Barbara, CA, 1998.
(14) Matsuzawa, M.; Potember, R. S.; Stenger, D. A.; Krauthamer, V. J. *Neurosci. Methods* **1993**, *50*, 253.
(15) Guo, A.; Rife, L. L.; Rao, N. A.; Smith, R. E. *Cornea* **1996**, *15*, 210.
(16) Camesano, T. A.; Logan, B. E. *Environ. Sci. Technol.* **2000**, *34*, 3354.
(17) Jucker, B. A.; Harms, H.; Hug, S. J.; Zehnder, A. J. B. *Colloids Surf., B* **1997**, *9*, 331.
(18) Rijnaarts, H. H. M.; Norde, W.; Lyklema, J.; Zehnder, A. J. B. *Colloids Surf., B* **1999**, *14*, 179.
(19) Ong, Y.-L.; Razatos, A.; Georgiou, G.; Sharma, M. M. *Langmuir* **1999**, *15*, 2719.
(20) Simoni, S. F.; Harms, H.; Bosma, T. N. P.; Zehnder, A. J. B. *Environ. Sci. Technol.* **1998**, *32*, 2100.
(21) DiRienzo, J. M.; Nakamura, K.; Inouye, M. *Annu. Rev. Biochem.* **1978**, *47*, 481.

10.1021/la015695b CCC: $22.00
Published on Web 04/09/2002

or inhibited adhesion.[4] The elastic and mechanical properties of polymers can be probed via stretching experiments using the atomic force microscope (AFM) or similar instruments. Single-molecule force spectroscopy (SMFS) allows individual molecules to be temporarily adsorbed to an AFM tip and stretched. Typically, the molecule is bonded or grafted to a substrate on one end, or in the case of cell surface macromolecules, the cell is attached to a substrate and the polymers are free in solution. These stretching experiments are used to provide information on polymer elasticity and other physical and chemical properties.

Quantitative information regarding chain elasticity can be obtained using statistical mechanical, random walk formulations, that is, the freely jointed chain (FJC), the wormlike chain (WLC), the extensible FJC, or the extensible WLC model.[2−3,22−39] In the FJC model, the polymer is considered to be composed of n independent rigid segments, each of segment length a.[27] The persistence length in the WLC model is the length of a statistically straight segment in the polymer.[27] By fitting the experimental data to these models, a segment length or persistence length can be estimated. These models predict linear forces at low extensions, where the chains behave like entropic Hookean springs. At moderate extensions, nonlinear, non-Gaussian forces will be predicted.[40] At high stretches, the force rapidly diverges as the distance approaches the contour length of the chain. The chain has fewer possible configurations and hence less entropy at high stretches.

The first extensive studies of this kind were performed with DNA. DNA, a unique biopolymer due to its size and large persistence length (∼50 nm), has now been extensively studied using single-molecule force spectroscopy.[26,30,35,36,41,42] These experiments have demonstrated a strong-stretching regime when the end-to-end distance approaches the DNA contour length and shows evidence of wormlike chain (WLC) behavior.[26,30] When the elasticity of λDNA was directly measured by an AFM and laser tweezers,[30,41] a sharp transition was discovered from a low to high extension state at a force of ∼0.45 pN for the underwound molecules and ∼3 pN for the overwound ones, reflecting the formation of alternative structures in stretched, coiled λDNA molecules.[41] In similar experiments, single-stranded DNA molecules were stretched in the presence of salt. Deviations from FJC behavior were observed, suggesting that DNA has significant local curvature in salt solutions.[36] In addition, the AFM was used also to directly probe interaction forces between complementary single strands of DNA.[42] Adhesive forces between complementary 20-base strands fell into three distinct distributions at 1.52, 1.11, and 0.83 nN. These forces are associated with the rupture of the interchain interaction between single pairs of molecules involving 20, 16, and 12 base pairs, respectively.

SMFS and AFM were used to study other biopolymers, such as the polysaccharides xanthan[25,43,44] and dextran,[28,45] polysaccharides on living cells of *Aspergillus oryzae*,[3] and many other biopolymers[3,22,29,31−33,46−49] and synthetic polymers.[2,23,24,37,49−51] In SMFS experiments, native xanthan shows a plateau in the force−extension curve at 400 pN that is characteristic of hydrogen bonding and electrostatic interactions stabilizing the double helices of the xanthan structure. The transition is irreversible and is not seen for denatured (single helical) xanthan.[25] Dextran macromolecules show a characteristic transition at 700 nN.[28,52] Based on Monte Carlo simulations, this transition was attributed to the C_5-C_6 bond of the sugar ring flipping into a new conformation, elongating the monomer by 0.65 Å (∼10% of its length).[52]

Recently, the AFM was used to identify the components of mixtures of polysaccharides at the single-molecule level. The elasticity of certain polysaccharides is governed by force-induced conformational transitions of the pyranose ring. These transitions produce atomic fingerprints in the force−extension spectrum that are characteristic of the type of the glycosidic linkage.[34,52,53] The force spectrums of dextran, cellulose, amylose, and pullulan have been identified and serve as chemical fingerprints for these polysaccharides. This method can identify and distinguish individual polysaccharide molecules adsorbed on a surface at single-molecule resolution, which is not possible by any other spectroscopic technique.

In this study, the elasticity of bacterial surface polymers from *Pseudomonas putida* KT2442 was measured by single-molecule force spectroscopy in solvents spanning a range of polarity (water, formamide, methanol) and ionic strengths (water, 0.01 M KCl, 0.1 M KCl). The WLC and FJC models were used to estimate polymer persistence and segment lengths. Adhesion forces between the polymer chains and the AFM silicon nitride tip were compared in these solvents.

(22) Ortiz, C.; Hadziioannou, G. *Macromolecules* **1999**, *32*, 780.
(23) Butt, H.-J.; Kappl, M.; Mueller, H.; Raiteri, R. *Langmuir* **1999**, *15*, 2559.
(24) Hugel, T.; Grosholz, M.; Clausen-Schaumann, H.; Pfau, A.; Gaub, H. E.; Seitz, M. *Macromolecules* **2001**, *34*, 1039.
(25) Li, H.; Rief, M.; Oesterhelt, F.; Gaub, H. E. *Adv. Mater.* **1998**, *3*, 316.
(26) Marko, J. F.; Siggia, E. D. *Macromolecules* **1995**, *28*, 8759.
(27) Flory, P. J. *Statistical Mechanics of Chain Molecules*; Hanser Publishers/Oxford University Press: New York, 1988.
(28) Rief, M.; Oesterhelt, F.; Heymann, B.; Gaub, H. E. *Science* **1997**, *275*, 1295.
(29) Kellermayer, M. S. Z.; Smith, S. B.; Granzier, H. L.; Bustamante, C. *Science* **1997**, *276*, 1112.
(30) Smith, S. B.; Cui, Y.; Bustamante, C. *Science* **1996**, *271*, 795.
(31) Oberdörfer; Y.; Fuchs, H.; Janshoff, A. *Langmuir* **2000**, *16*, 9955.
(32) Janshoff, A.; Neitzert, M.; Oberdörfer, Y.; Fuchs, H. *Angew. Chem., Int. Ed.* **2000**, *39*, 3212.
(33) Benoit, M.; Gabriel, D.; Gerisch, G.; Gaub, H. E. *Nature Cell Biol.* **2000**, *2*, 313.
(34) Marszalek, P. E.; Li, H.; Fernandez, J. M. *Nature Biotechnol.* **2001**, *19*, 258.
(35) Bustmante, C.; Marko, J. F.; Siggia, E. D.; Smith, S. *Science* **1994**, *265*, 1599.
(36) Smith, S. B.; Finzi, L.; Bustamante, C. *Science* **1992**, *258*, 1122.
(37) Oesterhelt, F.; Rief, M.; Gaub, H. E. *New J. Phys.* **1999**, *1*, 6.1−6.11.
(38) Oberhauser, A. F.; Marszalek, P. E.; Erickson, H. P.; Fernandez, J. M. *Nature* **1998**, *393*, 181.
(39) Oesterhelt, F.; Oesterhelt, D.; Pfeiffer, M.; Engel, A.; Gaub, H. E.; Müller, D. I. *Science* **2000**, *288*, 143.
(40) Haupt, B. J.; Ennis, J.; Sevick, E. M. *Langmuir* **1999**, *15*, 3886.
(41) Strick, T. R.; Allemand, J.-F.; Bensimon, D.; Bensimon, A.; Croquette, V. *Science* **1996**, *271*, 1835.
(42) Lee, G. U.; Chrisey, L. A.; Colton, R. J. *Science* **1994**, *266*, 771.
(43) Li, H.; Rief, M.; Oesterhelt, F.; Gaub, H. E. *Appl. Phys. A* **1999**, *68*, 407.
(44) Capron, I.; Alexandre, S.; Muller, G. *Polymer* **1998**, *39*, 5725.
(45) Rief, M.; Fernandez, J. M.; Gaub, H. E. *Phys. Rev. Lett.* **1998**, *81*, 4764.
(46) Stokke, B. T.; Falch, B. H.; Dentini, M. *Biopolymers* **2001**, *58*, 535.
(47) Razatos, A.; Ong, Y.-L.; Boulay, F.; Elbert, D. L.; Hubbell, J. A.; Sharma, M. M.; Georgiou, G. *Langmuir* **2000**, *16*, 9155.
(48) Balnois, E.; Stoll, S.; Wilkinson, K. J.; Buffle, J.; Rinaudo, M.; Milas, M. *Macromolecules* **2000**, *33*, 7440.
(49) Camesano, T. A.; Abu-Lail, N. I. *Biomacromolecules*, submitted for publication.
(50) Senden, T. J.; di Meglio, J.-M.; Auroy, P. *Eur. Phys. J. B* **1998**, *3*, 211.
(51) Li, H.; Zhang, W.; Zhang, X.; Shen, J.; Liu, B.; Gao, C.; Zou, G. *Macromol. Rapid Commun.* **1998**, *19*, 609.
(52) Marszalek, P. E.; Oberhauser, A. F.; Pang, Y.-P.; Fernandez, J. M. *Nature* **1998**, *396*, 661.
(53) Marszalek, P. E.; Pang, Y.-P.; Li, H.; El Yazal, J.; Oberhauser, A. F.; Fernandez, M. *Proc. Natl. Acad. Sci. U.S.A.* **1999**, *96*, 7894.

Table 1. Effect of Solvent on Average Properties of Adhesion Peaks

solvent	dielectric const (ϵ) (ref 71)	mean pull-off distance (nm)[a]	range of pull-off distances (nm)	mean pull-off force (nN)
formamide	111	295 ± 212	<1−725	−0.25 ± 0.24
water	80.1	212 ± 211	<1−812	−0.46 ± 1.3
methanol	33	137 ± 125	<1−576	−1.1 ± 2.3
0.1 M KCl		68 ± 59	<1−229	−0.66 ± 1.4
0.01 M KCl		119 ± 90	<1−440	−0.46 ± 0.50

[a] Caution should be used in interpreting these mean and standard deviation values. The high standard deviation is caused by the polydispersity of the sample and is not due to experimental "error". In addition to these values, histograms may provide a more meaningful way to examine the trends among the solvents (cf. Figures 2 and 4).

Materials and Methods

Cultures. Bacteria that have been extensively investigated for their use in bioremediation were chosen. D. F. Dwyer (Department of Earth, Ecological and Environmental Sciences, University of Toledo, Ohio) provided the *P. putida* KT2442. This strain can degrade substituted aromatic compounds under appropriate conditions.[54−57] KT2442 cultures were grown in M9 buffer containing a mineral salt mixture, 5 mM benzoate, and 50 μg/L rifampicin.[58]

Sample Preparation. KT2442 cells were covalently bonded to clean, silanized glass as described elsewhere.[16] Slides were kept hydrated the entire time prior to AFM work under purified water (Milli-Q water, Millipore Corp.), which was replaced with the desired solvent (0.1 and 0.01 M KCl solutions were used to investigate the effect of the ionic strength on biopolymer conformation; formamide, water, and methanol were used to study the effect of solvent polarity on biopolymer conformation (Table 1)).

Polymer Characterization. The polymers were separated from the bacterial cells (grown until late exponential growth phase) by centrifugation for 15 min at 6000 rpm (DAMON/IEC HT centrifuge). The polymers were freeze-dried and kept in the refrigerator until use.

Zeta Potential. The charge density of KT2442 cells and KT2442 surface polymers was measured using a zeta potential analyzer (Zeta PALS, BIC). Measurements were performed 10 times and averaged, on late exponential phase bacterial cells, resuspended in 0.1 mM MES buffer (pH = 6.66). A 1000 ppm solution of the freeze-dried polymers was prepared in 0.1 mM MES buffer. The zeta potential of the polymers was also measured 10 times and averaged.

Polarimetery. The optical rotatory dispersion of the polymers was determined using a Perkin-Elmer 241 MC polarimeter. A 25 000 ppm polymer water solution was prepared from the freeze-dried polymer. The measurements were run at four different wavelengths using a sodium lamp (589 nm) and a mercury lamp (546, 436, and 365 nm), and the maximum measured value of optical rotation in degrees was reported. The accuracy in measuring the optical rotation was ±0.001°.

Force Analysis Using the AFM. Forces were measured between individual bacterial cells and silicon nitride cantilevers in different solvents using an AFM (Digital Instruments Dimension 3100 with Nanoscope III controller). Silicon nitride tips were purchased from Digital Instruments (DNPS tips). The spring constant for these tips was 0.13 ± 0.02 N/m, measured using the Cleveland method[59] and the correlation equations given in the DI software. To select a cell for analysis, an image was obtained in tapping mode of a portion of the glass slide. The tip was then positioned over the center of a bacterium, the rastering of the cantilever was stopped, the tapping was turned off, and a force measurement was performed. Triplicate measurements were performed on a single area of a bacterial cell. Measurements were made for at least five cells under each solvent.

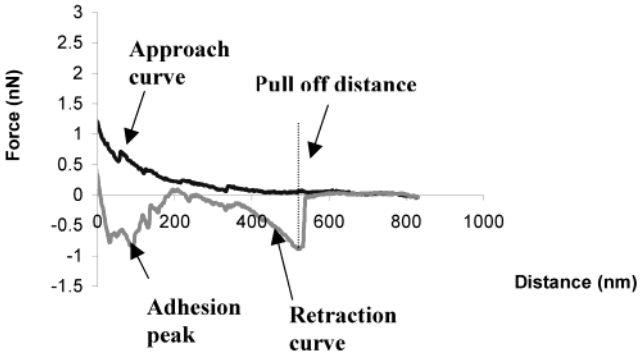

Figure 1. Typical AFM force curve. Far from the surface, there is no interaction between the polymer brush layer and the tip. As the tip approaches the surface, the polymer brush layer compresses, giving rise to a repulsive force. Often some of the surface polymers will attach to the tip once contact has been made, giving rise to the adhesion peaks in the retraction curve. Finally, the tip will detach from the polymers and the interaction force will return to zero.

The data files were treated as described previously[16] to convert them from AFM deflection data to force data, using the constant compliance region of the curves to "zero" the force curves.[60] Force measurements were also made on clean glass before and after force measurements on bacterial cells, to ensure that the tip was not contaminated during the course of the experiment. The measurements on glass were always identical (within the experimental error), confirming that the biopolymers were released as the tip was retracted.

Retraction Curves. Forces are recorded while the tip approaches and is retracted from the sample (Figure 1). Far from the sample surface, no forces are observed between the tip and bacterial polymers. As the tip approaches, the polymer brush layer compresses, inducing a repulsive force. Often when contact is made, polymers from the bacterial surface adsorb onto the tip. As the tip is retracted, a force equivalent to the adhesion force is required to pull the tip away from the polymer brush. This force is called the "pull-off force", and the location where it occurs depends on the length of the polymer chain. Multiple adhesion peaks may be observed, depending on the polymer type, the length of the polymer chain, and whether one or multiple chains are adsorbed to the tip.

Modeling. Three models were applied to the force−extension data. In the FJC model, the polymer is considered to be composed of n independent rigid segments, each of length a, connected by freely rotated pivots with equal probabilities for rotation in all directions. The chain gets more flexible as the segment length a gets smaller. The force needed to stretch a FJC to a length D is given by[23]

$$F_{\text{chain}} = \frac{-k_B T}{a} \mathrm{L}^{-1}\left(\frac{D}{L_c}\right) \quad (1)$$

where k_B is the Boltzmann constant (1.38106×10^{-23} J/K), T is absolute temperature, L_c is the polymer contour length, and L^{-1} is the inverse Langevin function, approximated by the first four terms of its series:[23]

$$\mathrm{L}^{-1} = 3\left(\frac{D}{L_c}\right) + \frac{9}{5}\left(\frac{D}{L_c}\right)^3 + \frac{297}{175}\left(\frac{D}{L_c}\right)^5 + \frac{1539}{875}\left(\frac{D}{L_c}\right)^7 \quad (2)$$

(54) Nüblein, K.; Maris, D.; Timmis, K.; Dwyer, D. F. *Appl. Environ. Microbiol.* **1992**, *58*, 3380.
(55) Lupi, C. G.; Colangelo, T.; Mason, C. A. *Appl. Environ. Microbiol.* **1995**, *61*, 2863.
(56) Van Der Meer, J. R.; Van Neerven, A. R. W.; De Vries, E. J.; De Vos, W. M.; Zehnder, A. J. B. *J. Bacteriol.* **1991**, *173*, 6−15.
(57) Schwartz, A.; Bar, R. *Appl. Environ. Microbiol.* **1995**, *61*, 2727.
(58) Camesano, T. A.; Unice, K. M.; Logan, B. E. *Colloids Surf., A* **1999**, *160*, 291.
(59) Cleveland, J. P.; Manne, S.; Bocek, D.; Hansma, P. K. *Rev. Sci. Instrum.* **1993**, *64*, 403.
(60) Ducker, W. A.; Senden, T. J.; Pashley, R. M. *Nature* **1991**, *353*, 239.

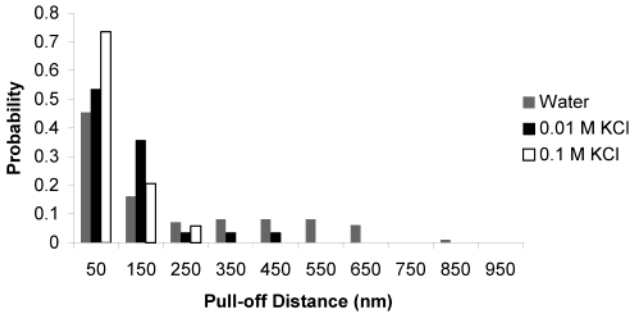

Figure 2. Probability distribution of pull-off distances for *P. putida* KT2442 biopolymers at different ionic strengths. The axis label corresponds to the center of the range.

Second, the WLC model was applied, in which the polymer chain is considered to be continuously curved and the direction of the curvature at any point in the chain is random. The chain in this model is intermediate between a rigid rod and a flexible coil. The WLC model takes into account the local stiffness of the chain in terms of the persistence length (L_P) and the long-range flexibility. The force required to stretch a wormlike chain in a solvent to a length D is given by[23]

$$F_{\text{chain}} = \frac{-k_B T}{L_P}\left[\frac{D}{L} + \frac{1}{4\left(1-\frac{D}{L_c}\right)^2} - \frac{1}{4}\right] \quad (3)$$

The extensible freely jointed chain model (FJC+) was used in some cases to account for elastic deformations of bonds and bond angles that are neglected in the freely jointed chain model. The polymer is modeled according to the FJC+ as n identical springs in series and can be expressed as[32]

$$D(F) = L_c\left[\coth\left(\frac{FL_k}{k_B T}\right) - \left(\frac{k_B T}{FL_k}\right)\right]\left[1 + \frac{F}{L_c \kappa}\right] \quad (4)$$

where L_k is the segment length, L_c is the contour length $= nL_k$, and κ is the spring constant of a single segment.

The model's ability to fit the experimental data was compared based on the estimated values of R^2 (the coefficient of determination, often used to judge the adequacy of a regression model) using the Tablecurve fitting program.

Results

Effect of Salt Concentration on Biopolymer Conformation and Adhesive Forces. Pull-off distances and adhesion forces between bacterial polymers and the silicon nitride tip were compared for all solvents. In water, a range of pull-off distances was observed up to 850 nm, with the mean at 212 nm (Table 1, Figure 2). While short polymers (<150 nm) were seen to a significant extent in all solvents, long polymers were not observed when salt was present. Over 70% of the pull-off distances were <50 nm in the highest salt solution (0.1 M KCl), while the percentages of polymers of this size were ~55% in 0.01 M KCl and ~45% in water. Polymers with pull-off distances of >450 nm were never observed in the salt solutions (Figure 2, Figure 3). These results indicate that the biopolymer was more elongated in pure water and could adopt a more coiled conformation when salt was present. The pull-off distances in water were compared to the pull-off distances in the other four solvents. In each case, the pull-off distances in water were statistically different from the pull-off distances in the other solvents (methanol, formamide, 0.01 M KCl, and 0.1 M KCl, each considered separately; statistical differences were determined by Mann−Whitney rank sum tests, all P values were <0.01).

No trend could be observed in the adhesion force with respect to electrolyte concentration (Table 1, Figure 3). The mean adhesion force was nearly the same in water, 0.1 M KCl, and 0.01 M KCl, within the range of experimental values observed.

Effect of Solvent Polarity on Biopolymer Conformation and Adhesive Forces. The average pull-off distance increased with increasing dielectric constant, with average distances of 137, 212, and 295 nm in methanol, water, and formamide, respectively (Figure 4). The polymers were clustered at shorter pull-off distances less in the more polar solvents, with the percentage of pull-off distances of <200 nm being 40% for formamide, 60% for water, and 80% for methanol (these distances were shown to be statistically different among solvents using a Mann−Whitney rank sum test, all P values were <0.01).

Solvent polarity also affected the adhesion force, with the highest affinity between the biopolymers and the tip observed in the least polar solvent (methanol; Figure 4, Figure 5). Generally in water and formamide, the adhesive interactions between the biopolymer and the AFM tip were similar, given the wide range of adhesive forces observed (Figure 5). However, at short distances (<88 nm), greater adhesion was observed in water compared to formamide (Figure 5).

Comparison with Polymer Elasticity Models

The Effect of Solution Ionic Strength. Salt solutions with concentrations of 0.01 and 0.1 M KCl were used to demonstrate the effect of solvent ionic strength on biopolymer conformation, and estimation of elastic parameters was made using the FJC and WLC models. While a range of persistence and segment lengths was observed (Table 2), generalizations can be made. The maximum persistence length value increased with increasing ionic strength, from 0.20 nm in 0.01 M KCl to 0.36 nm in 0.1 M KCl, indicating that the polymers become stiffer at higher salt concentrations (Figure 6, Table 2). The FJC model predicted the same trend, with a segment length up to 0.32 nm in 0.01 M KCl and 0.65 nm in 0.1 M KCl (Figure 7, Table 2).

The estimated contour lengths from the WLC model were shorter than the pull-off distances (~52−92% of the pull-off distance). The estimated contour lengths using the FJC model were longer than the pull-off distances in most cases.

Effect of Solvent Polarity. The WLC and FJC models were applied to the data in all solvents. The effect of solvent polarity on polymer conformation was probed by estimating the persistence (or segment) length and contour lengths in solvents with different dielectric constants: methanol, water, and formamide. Again, while a range of values was observed, some general trends are apparent. Using either model, the polymer was stiffer in more polar solvents. The maximum estimated persistence lengths based on the WLC model were 0.82 nm in formamide, 0.28 nm in water, and 0.21 nm in methanol (Figure 8). The FJC model predicted segment lengths up to 1.0 nm in formamide, 0.35 nm in water, and 0.18 nm in methanol (Figure 9, Table 2).

The estimated contour lengths using the WLC model were always less than the experimental pull-off distances (Table 2). Contour lengths between 31% and 93% of the pull-off distance were estimated in formamide, 29−99.6% in water, and 47−97% in methanol. More than 81% of the chains in all solvents were stretched to 85% of their pull-off distance, which is proportional to the contour length of the polymers.[37] Lower stretching capacities were observed at low and high extensions (Figure 8A−C).

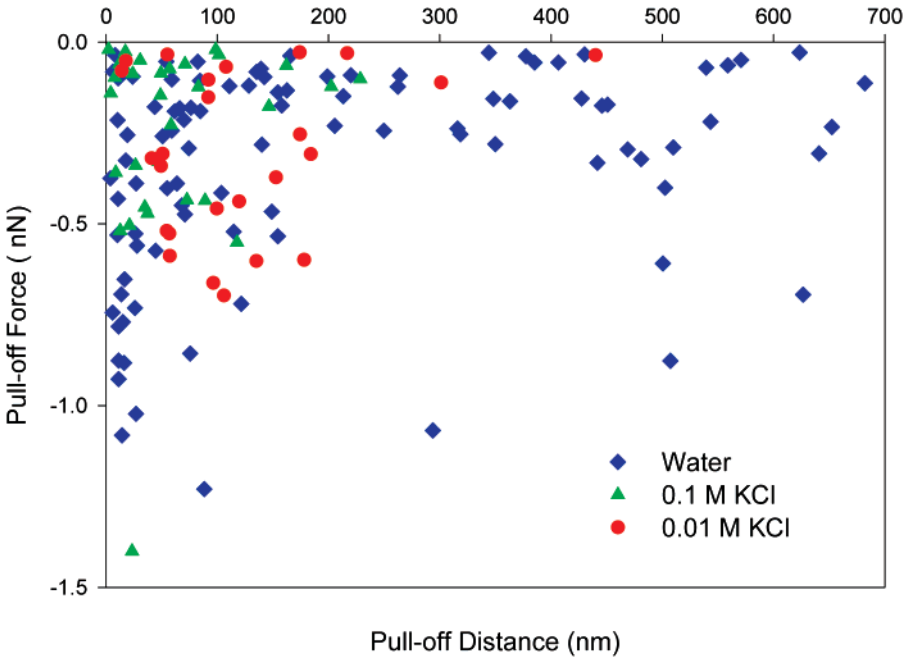

Figure 3. The pull-off force vs the pull-off distance for *P. putida* KT2442 biopolymers in different solvents, demonstrating the effect of ionic strength.

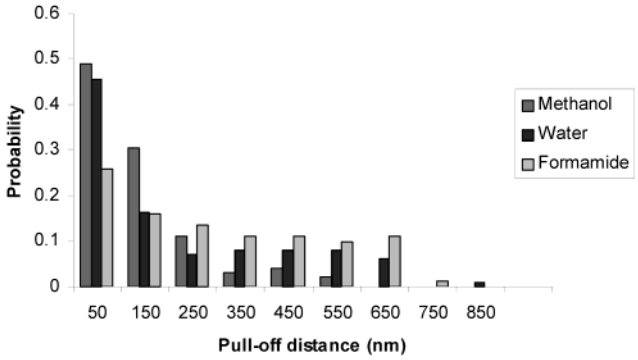

Figure 4. Probability distribution of pull-off distances for *P. putida* KT2442 biopolymers in solvents with different polarities. The axis label corresponds to the center of the range.

The estimated contour lengths using the FJC model usually exceeded the experimental pull-off distances. In formamide, contour length values between 49% and 133% of the pull-off distance were observed, while the percentages were 34−149% in water, and 52−132% in methanol. Since the contour lengths of these biopolymers are not known independently and we do not know if the entire biopolymer molecule was picked up by the AFM tip in each stretching event, we cannot speculate as to whether we have under- or overstretched chains.

Comparison of WLC and FJC Models. In comparing the two models for all solvents, the FJC model gives slightly better agreement with the experimental data ($R^2 = 0.86 \pm 0.20$ in FJC, $R^2 = 0.76 \pm 0.22$ in WLC). In addition, there were two cases where the WLC model could not be used. For chain extensions of <11 nm, the WLC model was discounted since it predicted persistence length values lower than the C−C bond length (0.154 nm). Also, at high-magnitude forces (>0.5 nN) and low chain extensions, the WLC model could not fit the whole range of the data (Figures 6A,B and 8B,C). The FJC model was able to fit all of the experimental data, for all of the solvents. Therefore, the FJC model is preferred since it applies to the whole range of data.

Extensible Freely Jointed Chain Model. Since the FJC model does not account for bond deformation or stretching of the molecules beyond their contour lengths, the FJC+ model was applied to force curves in water, to determine if these additional stretches needed to be accounted for. The FJC+ model has an additional enthalpic term that gives rise to a linear increase in the force for large extensions ($D \sim L_c$) and an additional fitting parameter that takes into account chain elasticity. The resulting fits for the FJC and FJC+ models are compared in water (Figure 10). In general, both models are in good agreement with the experimental data. At low extensions, the FJC works better than the FJC+ model, as shown by the higher R^2 values. At midrange extensions, both models can fit the data equally well. At high extensions, the FJC+ could not explain the experimental observations, since the experimental measured forces become small in value. The segment lengths estimated with the FJC+ model were 0.21−0.93 nm, which are higher than the segment lengths estimated using the FJC model (0.154−0.36 nm). The range of contour lengths was comparable using the two models, 7.5−838 nm with the FJC+, and 8.7−802 nm with the FJC model (for the same experimental data). The FJC+ model predicted segment elasticity values between 0.43 and 100 N/m for these biopolymers.

Discussion

Effect of Polarity and Ionic Strength on Biopolymer Conformation. While a range of segment and persistence lengths was observed in all solvents, the polymers were slightly more rigid in 0.1 M KCl compared to the lower salt or pure water solutions. The contour length of the biopolymers decreased when salt was added, probably because the macromolecules could adopt a more coiled conformation.

These types of transitions with respect to ionic strength (stiffer and more coiled when salt is present) are not uncommon. Many polysaccharides need some salt to be present in solution to stabilize their structures and will denature when no salt is present. For example, succinoglycan forms a disordered nonhelical structure in pure water but transforms to a gel-like structure in 0.1 M KCl.[49]

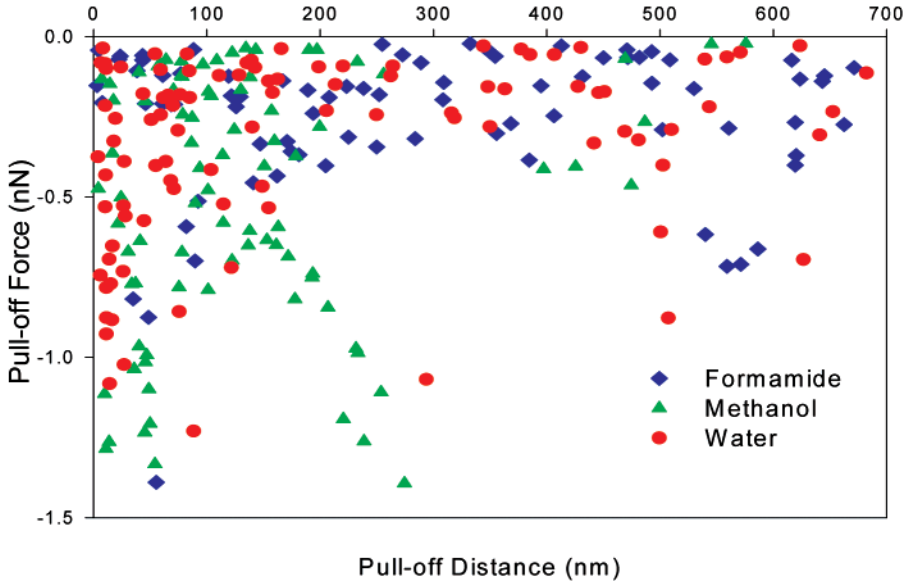

Figure 5. The pull-off force vs the pull-off distance for *P. putida* KT2442 biopolymers in different solvents, demonstrating the effect of solvent polarity.

Table 2. Summary of Model Parameters for Surface Biopolymers of *Pseudomonas putida* KT2442

	FJC			WLC		
solvent	L_c (nm)	a (nm)	mean R^2	L_c (nm)	L_P (nm)	mean R^2
water	9−1500	0.154−0.35	0.92 ± 0.13	9−1762	0.009−0.28	0.84 ± 0.17
formamide	4−853	0.154−1	0.84 ± 0.23	9−986	0.006−0.82	0.79 ± 0.19
methanol	8−1100	0.154−0.18	0.81 ± 0.22	7−1248	0.036−0.21	0.69 ± 0.21
0.1 M KCl	6−259	0.154−0.65	0.78 ± 0.32	7−300	0.154−0.36	0.67 ± 0.31
0.01 M KCl	6−176	0.154−0.32	0.88 ± 0.13	5−188	0.154−0.20	0.73 ± 0.21

Gel formation is possible because electrostatic repulsion between polymer chains is reduced in the present of salt. Denatured xanthan will renature into its native double-helix form only when salt is present.[61,62] Gellan is a double-stranded helix in very dilute aqueous solution containing low molecular weight salts but adopts a disordered, perhaps single-stranded configuration in the absence of added salts.[63] The presence of salts minimizes electrostatic repulsion among charged segments of the polysaccharide chains.

For charged polysaccharides in which electrostatic repulsion among subunits is strong, their conformation may be able to change from extended to coiled upon the addition of salt. For a polysaccharide produced by the marine bacterium *Pseudomonas atlantica*, as the ionic strength was increased to marine salt concentrations (about 0.5 M), adsorbed anionic EPS contracted in its configuration and collapsed onto the solid substrate surface.[64] As another example, the conformation of (negatively charged) xanthan chains transformed from isolated extended rods to coils and sometimes aggregates when KCl was added to solution.[61]

The estimated values of segment and persistence lengths for KT2442 polysaccharides are similar to values observed for other flexible polymers. SMFS experiments demonstrated a Kuhn length (segment length) of 6 ± 0.5 Å for dextran.[28] Poly(methacrylic acid), poly(dimethylsiloxane), and polyinosine all have segment lengths between 0.25 and 0.33 nm[22,42,48] (measured in SMFS experiments). However, some polysaccharides are much more rigid, such as xanthan[61] (L_P can be hundreds of nanometers, depending on whether salt is present), succinoglycan[49] (L_P = 36−105 nm, depending on whether salt is present), and scleroglucan[65,66] (L_P = 80 ± 10 nm).

Biopolymer Elastic Properties. Almost 70% of the chains in all solvents have persistence and/or segment lengths of 0.154−0.2 nm, which is only slightly higher than the C−C bond length (0.154 nm). This indicates that the polymers are flexible chains under all solvents.

Comparison between Different Models. Three different statistical models were used to fit the experimental data, the FJC, the WLC, and the FJC+. The first two models have two fitting parameters (contour length and either segment (FJC) or persistence (WLC) length). The FJC+ also includes a term for segment elasticity. At higher forces, chain segments are no longer oriented in a random fashion but orient predominately along the direction of the external force. The general polymer models, FJC and WLC, can describe this situation. The FJC model accounts only for entropic behavior. In the WLC model, enthalpic and entropic contributions are included, but extension is limited to the contour length of the polymer.[32]

The FJC model describes the experimental data for the KT2442 surface polymers very well, with a mean R^2 value of 0.86 ± 0.20. The FJC model has been successfully applied to many flexible polymers.[22,42,48] The WLC model was almost as good as the FJC model for most of the data, with an average R^2 value of 0.76 ± 0.22. However, the WLC model failed in two instances. At short distances, the WLC model predicted a persistence length shorter than the length of a C−C bond. There is some ambiguity in where to set the zero position in these force−extension

(61) Camesano, T. A.; Wilkinson, K. J. *Biomacromolecules* **2001**, *2*, 1184.
(62) Holzwarth, G.; Prestridge, E. B. *Science* **1977**, *197*, 757.
(63) McIntire, T. M.; Brant, D. A. *Biopolymers* **1997**, *42*, 133.
(64) Frank, B. P.; Belfort, G. *Langmuir* **1997**, *13*, 6234.
(65) Stokke, B. T.; Brant, D. A. *Biopolymers* **1990**, *30*, 1161.
(66) Vuppu, A. K.; Garcia, A. A.; Vernia, C. *Biopolymers* **1997**, *42*, 89.

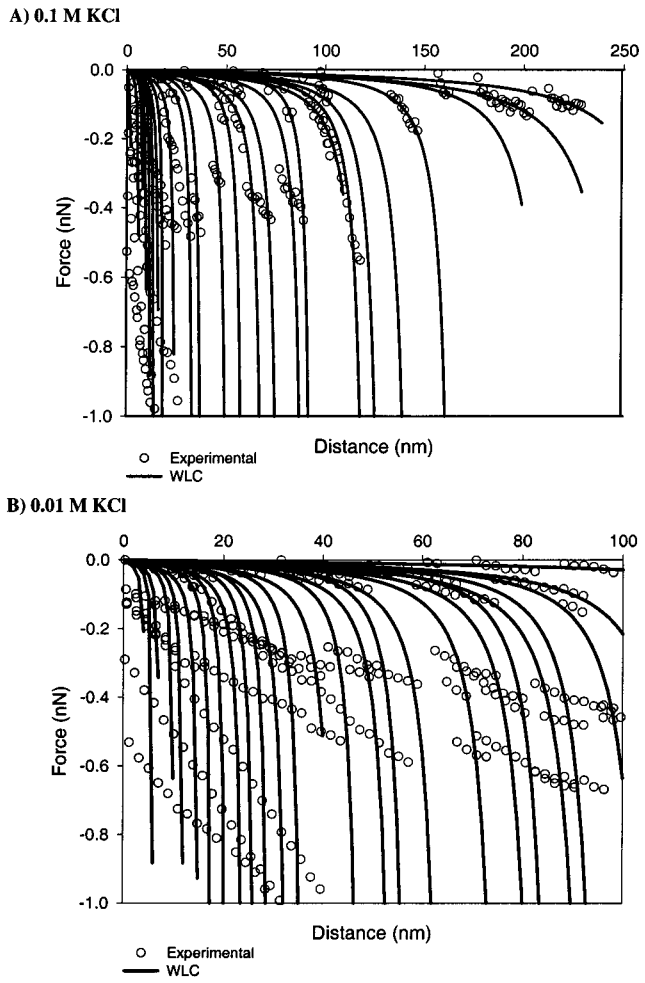

Figure 6. Comparison between experimental data and WLC model for KT2442 in (A) 0.1 M KCl (L_c = 6.8−300 nm, L_P = 0.154−0.36 nm, $R^2 = 0.67 \pm 0.31$. For all of the data in 0.01 M KCl, L_c is 1.16 ± 0.25 of the pull-off distance) and (B) 0.01 M KCl (L_c = 4.9−188 nm, L_P = 0.154−0.20 nm, $R^2 = 0.73 \pm 0.21$. In 0.01 M KCl, L_c is 1.14 ± 0.20 of the pull-off distance). Each solid line presents a stretching event of a polymer or a part of it and has its own persistence length and contour length that differ from those of other solid lines. The same applies to Figure 8.

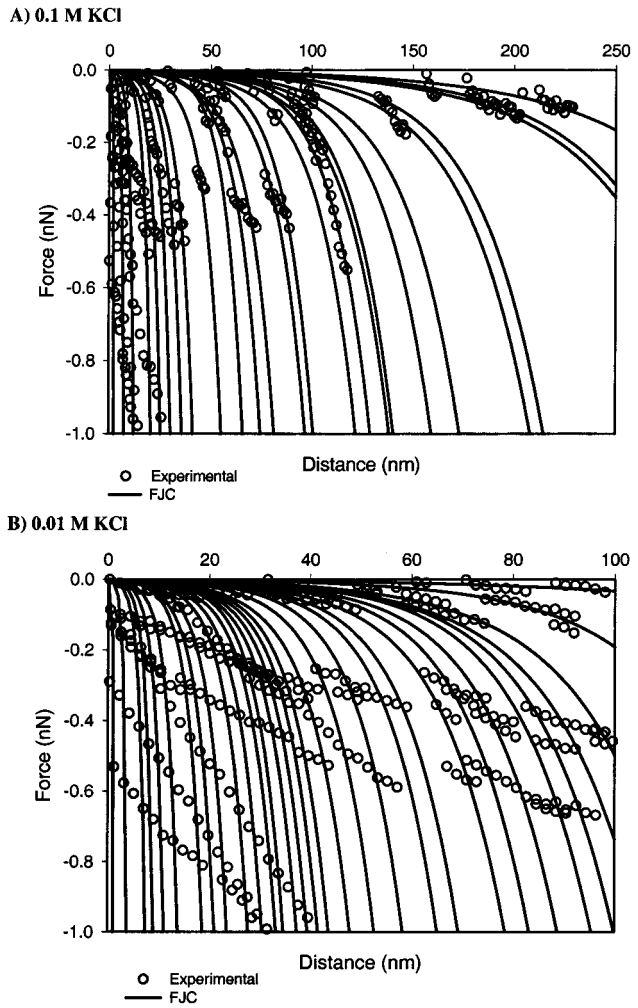

Figure 7. Comparison between experimental data and FJC model for KT2442 in (A) 0.1 M KCl (L_c = 5.7−259 nm, a = 0.154−0.65 nm, $R^2 = 0.78 \pm 0.32$. L_c in 0.1 M KCl is 0.90 ± 0.2 of the pull-off distance) and (B) 0.01 M KCl (L_c = 5.6−176 nm, a = 0.154−0.32 nm, $R^2 = 0.88 \pm 0.13$. L_c in 0.01 M KCl is 0.81 ± 0.19 of the pull-off distance). Each solid line presents a stretching event of a polymer or a part of it and has its own segment length and contour length that differ from those of other solid lines. The same applies to Figure 9.

curves, since the bacterial cell is slightly deformable. However, we estimate that our accuracy in establishing the zero positions for force and distance are within 10 nm and 0.06 nN, and so only minimal errors would be caused by this problem. In addition, the WLC model was less able to fit high-magnitude forces at low extensions (Figures 6A,B and 8B,C). Therefore, the FJC model is preferred over the WLC model for these particular biopolymers.

The FJC+ model takes into account elastic deformations by adding an enthalpic term to the FJC model. Segment elasticity represents the chains' ability to stretch beyond their contour lengths. This model works well at high forces, when a rupture in the bonds or a change in the structure is expected.[32] We tested the FJC+ model for our polymer chains in water, even though we have never observed plateau regions (indicative of conformational transitions) in our force−extension curves. The FJC+ was successfully applied to the data for the polymer chains in water in the low- to midrange extensions but did not fit our data well at higher extensions (Figure 10). Since the FJC+ model did not improve the fit compared to the FJC model, it is suggested that the polymers were not stretched beyond their contour lengths, and hydrogen bond rupture did not occur. The FJC+ model was not applied to the data for the other solvents, but we would expect a similar trend in the results.

Biopolymer Adhesion. Surface biopolymers may control bacterial adhesion.[1−5] In the present study, adhesion forces were measured between bacterial cells and an AFM tip in several solvents and adhesion was found to be a weak function of ionic strength. The adhesion forces were about the same in water, 0.01 M KCl, and 0.1 M KCl. The measured values of zeta potential for KT2442 bacterial cells (−17.31 ± 0.06 mV) and for the extracted surface polymers of KT2442 (−3.86 ± 0.04 mV) were quite different, indicating that the polymers have a low charge density. This may explain the weak dependence of the pull-off force on the ionic strength.

The effect of ionic strength on bacterial adhesion has been widely studied.[16,18,67] Less adhesion under low ionic strength conditions has been observed as a general trend. The decrease in adhesion is usually described by the classical Derjaguin−Landau−Verwey−Overbeek (DLVO)

(67) Camesano, T. A.; Logan, B. E. *Environ. Sci. Technol.* **1998**, *32*, 1699.

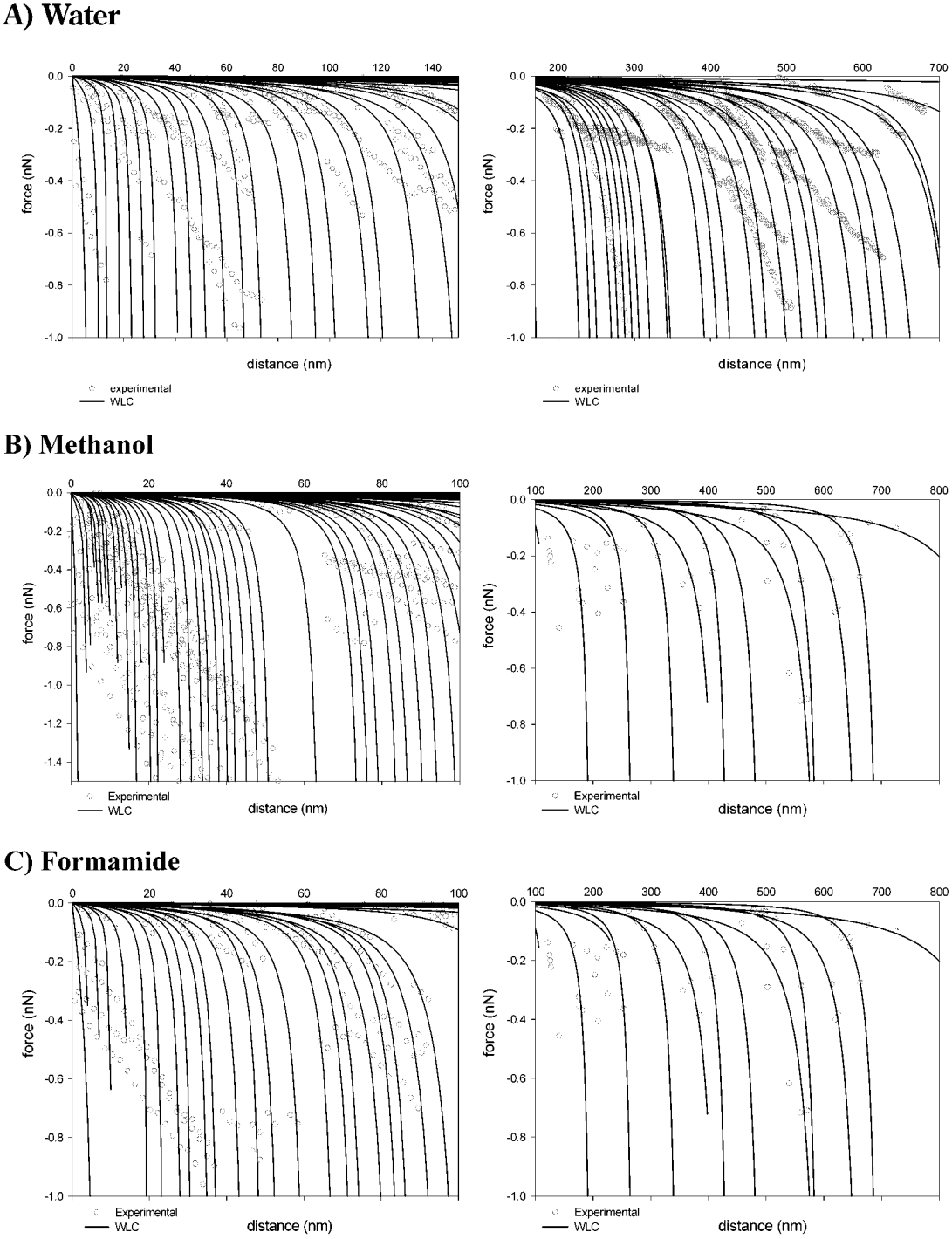

Figure 8. Comparison between experimental data and WLC model for KT2442 in (A) water ($L_c = 8.6-1762$ nm, $L_P = 0.009-0.28$ nm, $R^2 = 0.84 \pm 0.18$. L_c for all water lines is 1.18 ± 0.35 of the pull-off distance), (B) methanol ($L_c = 6.9-1248$ nm, $L_P = 0.04-0.22$ nm, $R^2 = 0.68 \pm 0.22$. L_c for all methanol data is 1.19 ± 0.46 of the pull-off distance), and (C) formamide ($L_c = 8.6-986$ nm, $L_P = 0.006-0.82$ nm, $R^2 = 0.79 \pm 0.19$. L_c for formamide is 1.19 ± 0.36 of the pull-off distance). For clarity, each curve is divided into two parts, showing the comparison between the experimental data and the WLC model at low and high extensions, separately.

theory of colloidal stability, in which the total interaction energy between two surfaces is considered as the sum of van der Waals and electrostatic interactions.[68] In bacterial adhesion studies, a transition sometimes occurs between a DLVO-controlled and a steric-controlled barrier to adhesion. The transition occurs at an ionic strength high enough for electrostatic interactions to be minimized.[18] Bacterial adhesion to porous media in transport studies has been found to be reduced in low ionic strength solutions,[51,67,69−70] although only qualitative agreement with predictions based on DLVO theory has been observed.[20]

In solvents with different polarities, adhesion was higher in the least polar solvent, methanol, and lower in the more polar solvents. The biopolymers are probably hydrophilic since they adhere more strongly to the tip

(68) Israelachivili, J. *Intermolecular & surface forces*, 2nd ed; Academic Press: San Diego, 1992.

(69) Gannon, J. T.; Tan, Y.; Baveye, P.; Alexander, M. *Appl. Environ. Microbiol.* **1991**, *57*, 2497.

(70) Fontes, D. E.; Mills, A. L.; Hornberger, G. M.; Herman, J. S. *Appl. Environ. Microbiol.* **1991**, *57*, 2473.

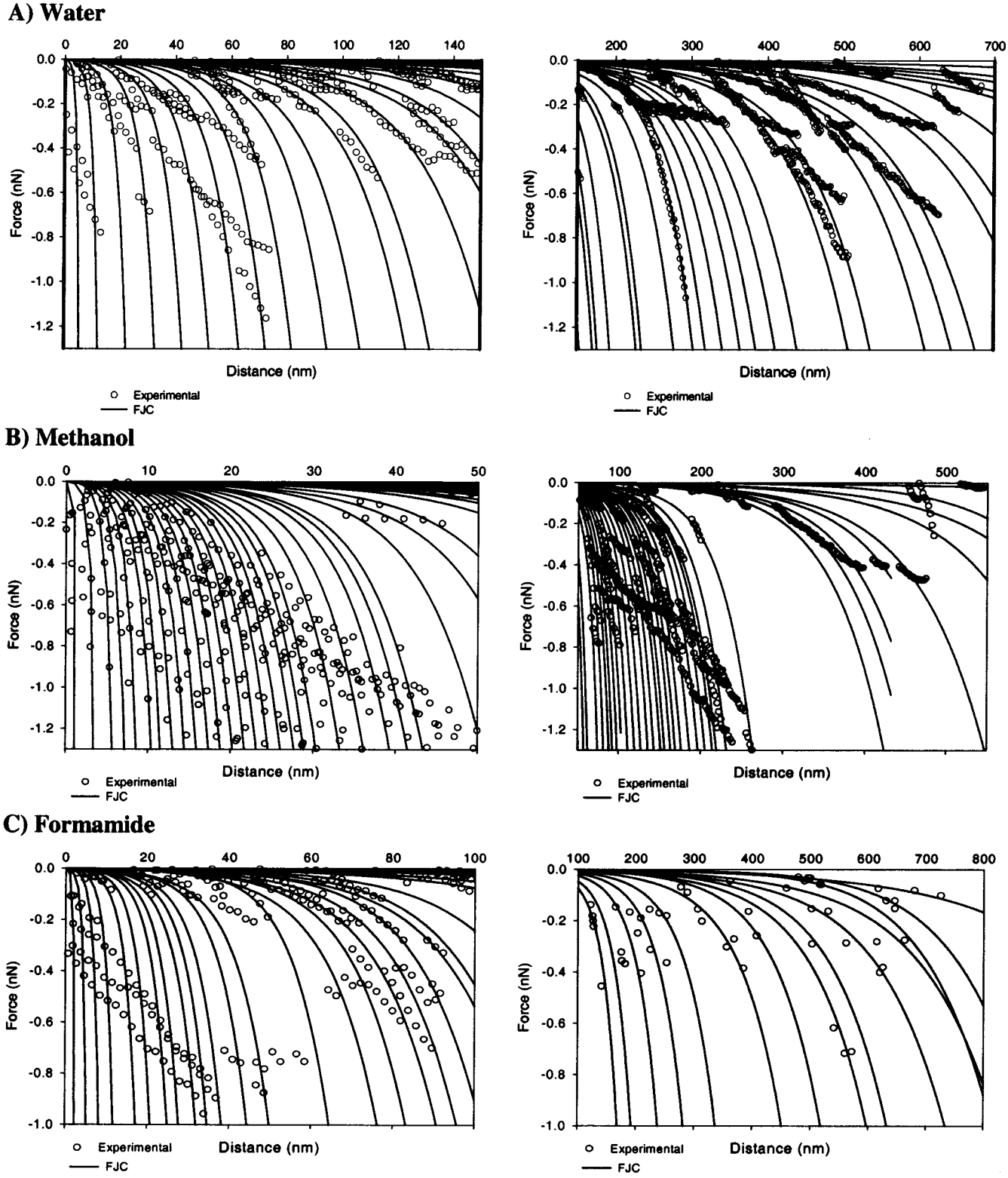

Figure 9. Comparison between experimental data and FJC model for KT2442 in (A) water ($L_c = 8.7-1500$ nm, $a = 0.154-0.35$ nm, $R^2 = 0.92 \pm 0.13$. L_c for all the data considered together is 0.91 ± 0.38 of the pull-off distance), (B) methanol ($L_c = 7.6-1100$ nm, $a = 0.154-0.18$ nm, $R^2 = 0.83 \pm 0.21$. L_c for all the data considered together is 0.82 ± 0.20 of the pull-off distance), and (C) formamide ($L_c = 3.9-853$ nm, $a = 0.154-1.0$ nm, $R^2 = 0.84 \pm 0.23$. L_c for all of the data considered together is 0.88 ± 0.26 of the pull-off distance). For clarity, each curve is divided into two parts, showing the comparison between the experimental data and the WLC model at low and high extensions, separately.

under the least hydrophilic conditions. Previous indirect evidence indicated that KT2442 produced hydrophilic polymers, since the water contact angle on a lawn of bacterial cells is 24.5°.[58] Other research has demonstrated that repulsion due to intrachain interactions decreases in less polar solvents. For example, hydrophobic intrachain interactions were eliminated in hexadecane, which is an entirely apolar solvent.[37] The nature of the solvent affects solvation forces and depends on the dielectric constant (ϵ) in a complex manner.[68]

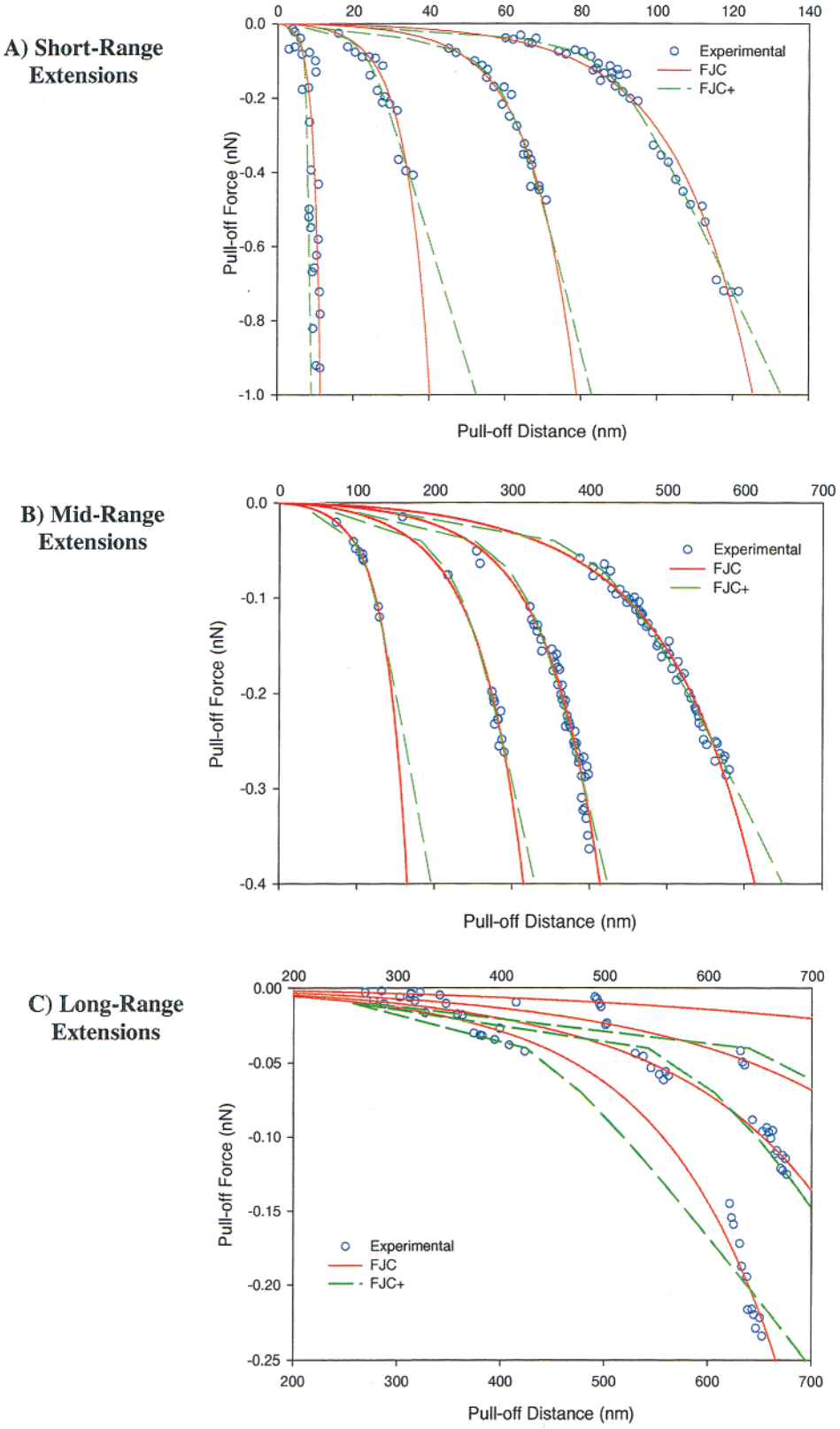

Figure 10. (A) Comparison between FJC and FJC+ models at low extensions in water (R^2 values range between 0.47 and 0.97 with FJC and from 0.39 to 0.97 with FJC+). (B) Comparison between FJC and FJC+ models at midrange extensions under water (R^2 values range between 0.94 and 0.99 in the FJC model, while they range between 0.97 and 0.99 in the FJC+ model). (C) Comparison between FJC and FJC+ models at high extensions under water (R^2 values range between 0.58 and 0.98 with the FJC model, while the FJC+ was not able to fit the last curve). L_c for all of the data considered together is 0.80 ± 0.19 of the pull-off distance.

Heterogeneity of Biopolymers. In our study, a range of values of segment lengths, persistence lengths, and contour lengths was observed, which seems to indicate that more than one type of polysaccharide is present on the bacterial surface. The range of contour lengths is not surprising, and care must be taken in interpreting these data since the tip may make contact with some point along the chain that is not necessarily the end of the chain. The

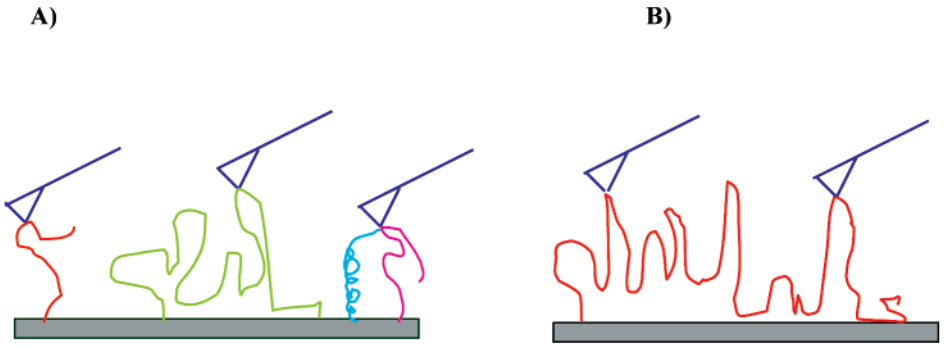

Figure 11. (A) Different polymers apparently exist on the surface of *P. putida* KT2442. More than one type can be attached to the tip at the same time. (B) A surface polymer on KT2442 that can be attached to the tip at different locations. Even though multiple polymers (or portions of polymers) may attach to the tip as the tip approaches the surface, the chains will detach at different times. Therefore, when we analyze each adhesion event in our force−extension spectra, we are always examining the detachment (i.e., adhesion) of a single chain.

lengths observed cannot be easily related to the actual length of the polymer (Figure 11). In other studies on well-defined biopolymers, where the contour length is clearly known, all the data can be normalized to the contour length of the polymer.[22,24,25] We cannot normalize the data by the length since the polymer length is not independently known. However, even if we cannot be sure how many different length polymer molecules are present on the bacterial surface, it still appears that we have multiple types of polymers based on the range of different persistence and segment lengths observed. If the biopolymer material were chemically homogeneous but of different lengths, the persistence length would not be expected to change.

Based on a size exclusion chromatography (SEC) experiment on extracted biopolymers from *P. putida* KT2442, a broad peak was observed near a polymer molecular weight of 1.8×10^5. The broadness of this peak indicated that multiple sized polymers are present (data not shown).

Chemical Nature of the Biopolymers. The AFM provides primarily physical information but has recently been used as a chemical "fingerprinting" technique for certain polysaccharides.[34] Researchers have shown that bond linkages in α (1→4) sugars often give rise to characteristic and reproducible transitions in SMFS experiments. For example, amylose and dextran each show single transitions that occur at ∼280 and ∼850 pN, respectively. Some polysaccharides, such as pectin, show two transitions in their force spectra, due to a two-step chair inversion transition in the α-D-galactopyranuronic acid ring. A technique has now been developed for relating the number of conformational transitions in force spectrograms to the sum of the glycosidic and aglycon bonds in the axial (a) position. One polysaccharide that does not show a force transition is methylcellulose (a sugar with β-linkages), which displays purely entropic behavior. The force spectra we observe for *P. putida* KT2442 biopolymers most closely resemble those of cellulose, since no transition is observed that could be attributed to a conformational transition. Also, the purely entropic FJC model is able to represent the elastic properties of these biopolymers quite well. A polarimetry test run on our polymers confirmed this hypothesis. The negative rotations observed in the measurements indicated that we have a β sugar.[72] Determining detailed chemical information on polysaccharides would require the use of the AFM in combination with other methods. However, new techniques such as polysaccharide fingerprinting or the use of chemically modified tips allow the AFM to provide an unprecedented degree of chemical information at a molecular level on microbial and other cell surfaces.

(71) *Handbook of chemistry and physics*, 81st ed; Lide, D. R., Ed.; CRC Press: Boca Raton, FL, 2000−2001.

(72) Robyt, J. F.; White, B. J. *Biochemical Techniques, Theory and Practice*; Waveland Press: Prospect Heights, IL, 1990.

Summary

Single-molecule force microscopy was successfully used to quantify the elasticity of *P. putida* KT2442 polymers in various solvents. The effect of ionic strength on the polymer elasticity was studied through use of 0.1 and 0.01 M KCl solutions. The effect of polarity on polymer elasticity was studied using methanol, water, and formamide. Three different models were used to quantify polymer elasticity from force−extension profiles: the freely jointed chain, wormlike chain, and extensible freely jointed chain models. The FJC was found to fit the experimental data better than the WLC model. Enthalpic effects were found to be unimportant; hence, the FJC+ was not better than the FJC model. The polymers are found to be very flexible, since more than 70% of the total estimated segment or persistence lengths of the chains is ∼0.18 nm, a little higher than the C−C bond length (0.154 nm). The adhesion forces are weakly dependent on ionic strength. This might be due to the low charge density of KT2442's surface polymers. Adhesion forces between the bacteria and the AFM tip increase as the polarity decreased, indicating that the polymers are hydrophilic. The KT2442 polymers were thought to be cellulose-like, based on their optical rotation and characteristic force spectra. This work will be useful to those wishing to develop improved models of bacterial adhesion. We have demonstrated the important effect of surface polymer properties on adhesion forces and point out the need for bacterial adhesion models to account for polymer properties and polymer heterogeneity.

Acknowledgment. We thank Jayne Morrow and Professor Domenico Grasso (Smith College) for their help in performing the zeta potential measurements, Dr. Rick Stock (WPI) for his help in purifying the bacterial polymers, Professors Lale Burk and Kate Queeney (Smith College) for their help in performing the polarimetry tests, and Professor William Hobey (WPI) for helping us interpret the polarimetry results.

LA015695B